Variable mass oscillator

José Flores
Departamento de Física "J. J. Giambiagi," Universidad de Buenos Aires, Argentina
and Facultad de Ingeniería y Ciencias de la Universidad Favaloro, Buenos Aires, Argentina

Guillermo Solovey
Departamento de Física "J. J. Giambiagi," Universidad de Buenos Aires, Argentina

Salvador Gil[a)]
Departamento de Física "J. J. Giambiagi," Universidad de Buenos Aires, Argentina,
Escuela de Ciencia y Tecnología de la Universidad Nacional de San Martín, Buenos Aires, Argentina,
and Facultad de Ingeniería y Ciencias de la Universidad Favaloro, Buenos Aires, Argentina

We studied the motion of a variable mass oscillator. The mass used is a container full of sand that loses sand at a constant rate and hangs from a spring. The spring was suspended from a force sensor connected to a data acquisition system that let us study the evolution of the system. In the underdamped regime we identified three distinct types of behavior for the system, depending on the relation between the energy loss due to the exit of mass and the energy loss through friction. The experimental results are well described by both the numerical solution to the equations of motion and our model, which makes it simple to predict the different types of behavior and to assess the relevant physical parameters involved in the dynamics of this system. © *2003 American Association of Physics Teachers.*
[DOI: 10.1119/1.1571838]

I. INTRODUCTION

Variable mass systems are seldom discussed in introductory physics courses, but offer an interesting and instructive perspective on Newton's second law.[1–3] We present a simple, inexpensive, and novel device that can be easily constructed and used with introductory and intermediate students of mechanics. We address the question of how the natural frequency ω of a harmonic oscillator changes with time if the mass of the system varies. In particular, we determine if the relation

$$\omega = \sqrt{\frac{k}{m}}, \qquad (1)$$

where k is the spring constant and m is the mass of the system, remains valid if the mass is variable, that is, if $m = m(t)$.[4]

As discussed in Ref. 5, the flow of a granular material through an opening is constant in time, regardless of the height of the column of the granular material in the container.[5,6] The constant flow rate property of granular materials lets us study the case in which the mass of the oscillator decreases linearly with time. Furthermore, because the flow rate of granular materials depends on the area of the opening,[6,7] we can control the flux of sand.

II. EXPERIMENTAL SETUP

The experimental setup consists of an inverted plastic soda bottle filled with sand and hung from a spring, which in turn is suspended from a force sensor connected to a data acquisition system, as illustrated schematically in Fig. 1. We used openings of different sizes in the lids of the bottle to study the behavior of the oscillator for different flow rates. To characterize the variation of the mass with time and measure the flux rate, we simply hung the bottle from the force sensor

and measured $m(t)$. Because the geometrical shape of the system is the same, so is the friction force for all the flow rates used.

Because the container is accelerating, it is not obvious that the flow rate will still be constant. To study this issue experimentally, we hung the spring with the bottle from a fixed point. Then we hung a bucket from the sensor that was placed below the oscillating bottle (see Fig. 2). In this manner we were able to compare the flux rate when the bottle was still and when it was oscillating (Fig. 2).

III. EXPERIMENTAL RESULTS

Using the setup illustrated in Fig. 2 (upper panel), we studied whether the flow rate changed during the oscillations of the bottle. We detected no change in the flow rate during the oscillation of the system. Figure 2 (lower panel) shows a typical result. The slopes in both cases (bottle oscillating and stationary) are the same. We performed a fast Fourier transform (FFT) on the data for $m(t)$ and $dm(t)/dt$ and searched for components of the FFT that corresponded to the frequency of the oscillation or its harmonics and found no correlation. We thus conclude that, within the sensitivity of our system (5%), there is no change in the flow rate for either case. This result is not trivial, because if the bottle were falling with an acceleration g, the local acceleration of gravity, we would expect the flow rate to be zero. In our case the maximum values of the oscillator acceleration were much less than g with $\langle a(t) \rangle \approx 0$. This result justifies our observation that the flow rate is independent of whether the bottle was stationary or oscillating.

By using different lids, we studied the behavior of the oscillator for different flow rates. We observed three distinct types of behavior according to the flow rate as illustrated in Fig. 3. Figure 4 illustrates the variation of the period $T = 2\pi/\omega$ as a function of time. We observed that ω was well
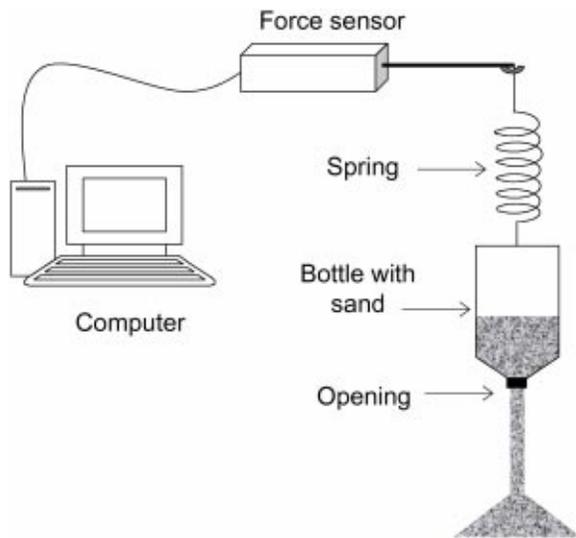
Fig. 1. Schematic of experimental setup. The spring is hung from the force sensor which is connected to a data acquisition system. The bottle with sand is the variable mass system. Lids with different size openings are used to study oscillations for different flow rates.

described by the relation $\omega^2 = k/m(t)$. This result will be a useful bench mark to further constrain the theoretical models.

IV. THEORETICAL CONSIDERATIONS

The equation of motion for a variable mass system that loses mass at a rate $c = -dm(t)/dt$, such that the mass leaves the container with a velocity q relative to it, can be written as[5,7]

$$F = \frac{P(t)}{dt} = M(t)\frac{dv}{dt} - q\frac{dM}{dt}. \tag{2}$$

We assume that the relative velocity, q, of the sand, at the moment it leaves the container is equal to zero. Consequently, there is no thrust in our case, and therefore

$$\frac{dP}{dt} = M(t)\frac{dv}{dt}. \tag{3}$$

The air drag friction force, F_f, of an object moving in a fluid at low velocities is proportional to the velocity, $F_f = -bv$, where the constant of proportionality b depends on the geometry of the object and the viscosity of the fluid.[8] The parameters k and b can be measured independently.[9]

According to Eq. (3), the equation of motion for our system is

$$m(t)\frac{d^2x}{dt^2} + b\frac{dx}{dt} + kx = 0. \tag{4}$$

If we multiply Eq. (4) by dx/dt, we find

$$m(t)\frac{d^2x}{dt^2}\frac{dx}{dt} + b\frac{dx}{dt}\frac{dx}{dt} + k.x\frac{dx}{dt} = 0. \tag{5}$$

The derivative of the kinetic energy, E_k, of a variable mass system can be written as

$$\frac{dE_k}{dt} = \frac{1}{2}\frac{dm(t)}{dt}\left(\frac{dx}{dt}\right)^2 + m(t)\frac{dx}{dt}\frac{d^2x}{dt^2}. \tag{6}$$
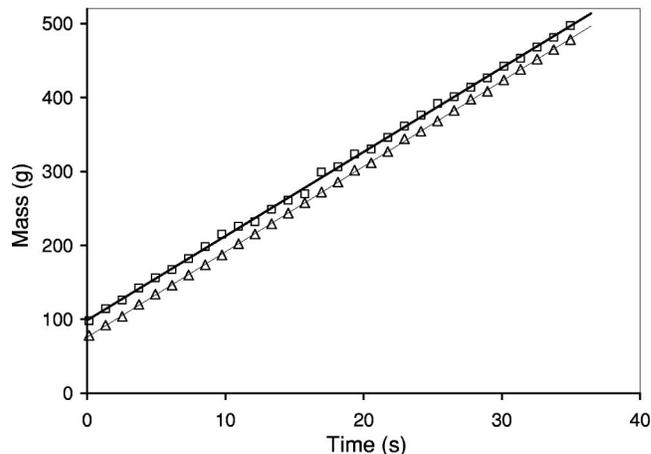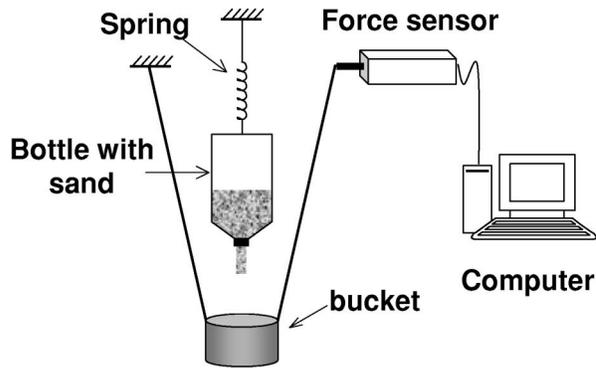
Fig. 2. Upper panel: Schematic diagram of experimental setup 2. The bucket is hung from the force sensor which is connected to a data acquisition system. By replacing the spring by a string, we can analyze whether there is any variation in the flux due to oscillations. Lower panel: Experimental data of the mass as a function of time. The triangles indicate the data for a fixed bottle and the squares are the corresponding data for an oscillating bottle. The flow rate remains constant and has the same slope in both cases. No correlation was found between the FFT spectrum of $m(t)$ and $dm(t)/dt$ and the frequency of oscillation of the bottle.

Because the potential energy of the spring is $E_p = 1/2k.x^2$, Eq. (5) can be written as

$$\frac{d(E_k + E_p)}{dt} - \frac{1}{2}\frac{dm(t)}{dt}\left(\frac{dx}{dt}\right)^2 + b\left(\frac{dx}{dt}\right)^2 = 0. \tag{7}$$

In our case $m(t) = m_0 - ct$, and $dm(t)/dt = -c$. Therefore, Eq. (7) becomes

$$\frac{d(E_k + E_p)}{dt} = -\left(b + \frac{c}{2}\right)\left(\frac{dx}{dt}\right)^2. \tag{8}$$

Equation (8) quantifies the energy loss of the system by friction and mass loss.[10] We can use Eq. (8) to determine the variation of the amplitude of the system with time. We shall express this amplitude as $A(t) = A_0 f(t)$. If we consider two consecutive oscillations, the time rate of energy loss can be written as

$$\frac{d(E_k + E_p)}{dt} = \frac{d}{dt}\left(\frac{1}{2}kA^2\right) \approx -\left(b + \frac{c}{2}\right)\langle v^2\rangle, \tag{9}$$

where $\langle v^2\rangle$ represents the mean square average of the velocity over a particular period and is estimated by $A^2\omega^2/2$, where ω is the angular frequency associated with the corresponding period. We can further approximate $\omega^2 \approx k/m(t)$,
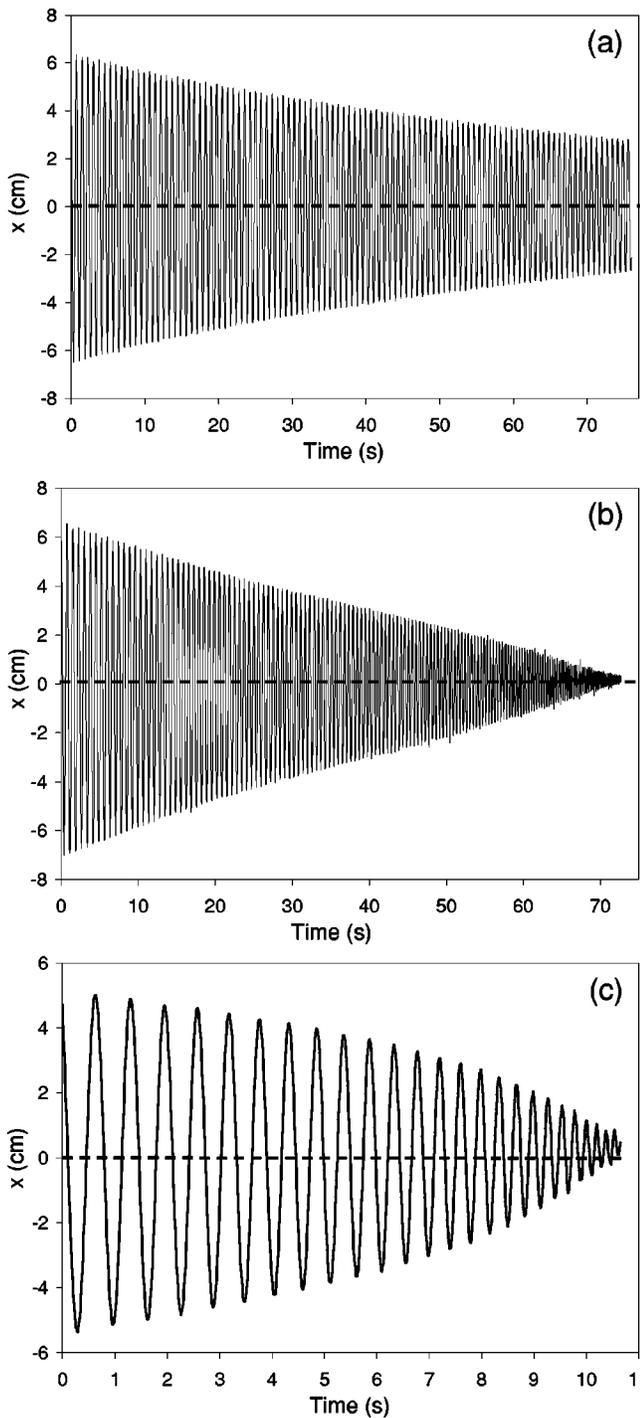
Fig. 3. Experimental variation of position, $x(t)$, as a function of time, for the three types of underdamped oscillations. The common friction coefficient is $b = 25$ g/s. (a) Typical behavior of the underdamped oscillations corresponding to low flow rate, $c = 2$ g/s and $\varepsilon \gg 1$. (b) The flow rate is $c = 15$ g/s and $\varepsilon \approx 1$. (c) Highest flow rate, $c = 90$ g/s and $\varepsilon < 1$. Notice the different time scale in the three cases, which scales with the mass flow rate.

which is consistent with our experimental observations (see Fig. 4). These approximations combined with Eq. (9) lead to

$$\frac{dA}{dt} \approx -\frac{1}{2}\left(b + \frac{c}{2}\right)\frac{A}{m(t)}. \tag{10}$$

The solution of Eq. (10) is
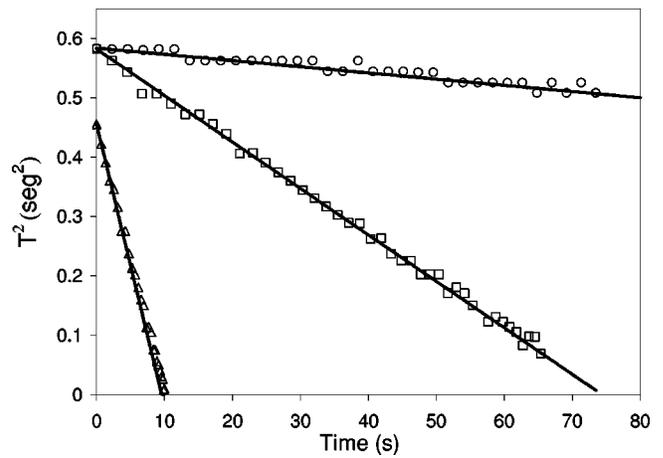
Fig. 4. Variation of the square of the measured period of oscillations, $T(t)^2$, as a function of the mass. The linear variation is clearly visible, in agreement with the prediction of Eq. (1). Circles represent data collected for $c = 2$ g/s flow rate ($\varepsilon \ll 1$), squares for $c = 15$ g/s ($\varepsilon \approx 1$), and triangles for $c = 90$ g/s ($\varepsilon < 1$).

$$A(t) = A_0 f(t) = A_0 \left(1 - \frac{ct}{m_0}\right)^{\varepsilon}, \tag{11}$$

with $\varepsilon = b/2c + \frac{1}{4}$. The term $b/2c$ represents the ratio of the energy loss by friction and the energy leaving the system due to the mass loss. Note that the concavity of the envelope, characterized by the sign of the second derivative of Eq. (11) depends on the value of ε. If $\varepsilon > 1$, $A''(t) > 0$ and the envelope is concave; the opposite is true if $\varepsilon < 1$, and for $\varepsilon = 1$ $A''(t) = 0$. If we consider the limit of Eq. (11) when $\tau = ct/m_0$ goes to zero (that is, $c \rightarrow 0$), we obtain

$$\lim_{\tau \to 0} A(t) = A_0 \exp\left(-\frac{b}{2m_0}t\right), \tag{12}$$

which is the well-known result for the variation of the amplitude with time for an underdamped harmonic oscillator. It is interesting to note that the limit $\tau \rightarrow 0$ means small fluxes or, equivalently, a time scale much smaller than m_0/c, that is, when the bottle is far from being empty.

There are two interesting special cases of Eq. (11):
(a) $\varepsilon = 1$ ($b/2c = \frac{3}{4}$) leads to

$$A(t) = A_0 \left(1 - \frac{ct}{m_0}\right). \tag{13}$$

In this case the amplitude decreases linearly with time, similar to the behavior illustrated in Fig. 3(b).
(b) $\varepsilon = \frac{1}{4}$ ($b/2c \ll 1$) leads to

$$A(t) = A_0 \left(1 - \frac{ct}{m_0}\right)^{1/4}. \tag{14}$$

Equation (14) represents the most convex envelope, that is, the second derivative of Eq. (14) is as negative as it can be. In this case the energy loss is dominated by the exiting mass. Figures 3 and 5 illustrate three distinct types of behavior and indicate how well our model describes the experimental data.

Now that we have obtained an adequate description of the amplitude, we will find an approximate solution to Eq. (2) by making the ansatz:

$$x(t) = A_0 f(t) \sin(h(t)). \tag{15}$$

Fig. 6. Comparison of the experimental result of $x(t)$ (open circles) for the case illustrated in Fig. 3(c), together with the prediction of our model (light solid line), Eq. (16). The agreement is excellent for all cases (different values of ε). The heavy solid line represents the envelope predicted by Eq. (11). When the bottle is running out of sand, we begin to see the limitation of the model, as would be expected from Eq. (18).

Fig. 5. Variation of the amplitude as a function of time. (a) Low flow rate case, $c = 2$ g/s ($\varepsilon \gg 1$) [Fig. 3(a)]. (b) $c = 15$ g/s ($\varepsilon \approx 1$) [Fig. 3(b)]. (c) $c = 90$ g/s ($\varepsilon < 1$) [Fig. 3(c)]. The circles represent the observed data obtained from the peaks of the oscillations. The numerical integration of Eq. (4) using MatLab is represented by triangles. The lines correspond to the prediction of our model, Eq. (11). The agreement among the numerical integration, our model, and the data is excellent.

If we substitute Eq. (15) in Eq. (4), we can find $f(t)$ and $h(t)$. The details are discussed in the Appendix. Thus, the solution to the differential equation (4) is

$$x(t) = A_0 \left(1 - \frac{ct}{m_0} \right)^{\varepsilon} \sin(h_0(t) + \phi), \tag{16}$$

where, as usual, the constants A_0 and ϕ are determined by the initial conditions of the system, and $h_0(t)$ is given by

$$h_0(\tau) = \frac{2.\beta}{c} \left[\arctan\left(\sqrt{\frac{1-\alpha-\tau}{\alpha}} \right) - \left(\sqrt{\frac{1-\alpha-\tau}{\alpha}} \right) \right]. \tag{17}$$

According to the Appendix, Eq. (16) is expected to be an adequate solution to Eq. (4) as long as the condition,

$$\frac{(b+c/2)(b+3c/2)}{4k} \ll m(t), \tag{18}$$

is satisfied. Therefore, we can expect our model to be inadequate when the bottle is close to running out of sand.

V. DISCUSSION

In Fig. 6 we present the experimental results of $x(t)$ together with the predictions of our model. In all the cases we studied, the agreement is quite good. Furthermore, we also compared the approximate solution of our model, Eq. (16), with the numerical integration of Eq. (4). Again, there is excellent agreement between these two approaches. We note that although the numerical integration of Eq. (4) is straightforward, it hides the physics, which in our approximate model, Eq. (16), is clearly apparent. For example, suppose that we wish to obtain an approximate expression for the variation of the period of the system with time, $T(t)$. We define the period as the time interval over which the phase changes by 2π, that is, from Eq. (A5),

$$\int_{t}^{t+T} h'(\tau) \, d\tau \approx h'(t) T(t) = 2\pi. \tag{19}$$

Therefore, using Eq. (1) for the frequency, we obtain

$$T^2(t) \equiv \frac{4\pi^2}{\omega^2(t)} \approx 4\pi^2 \frac{m(t)}{k}. \tag{20}$$

This connection between the period and the mass is clearly illustrated in Fig. 4, which also shows the advantages of having a model. Finally, our model also helps us to interpret the physics behind the change in shape of the envelope of the oscillator according to the magnitude of the flow rate. As discussed, the total energy of the system is related to the amplitude $A(t)$ of the oscillation according to Eq. (9). The rate of energy loss of the system depends on two mecha-

nisms: friction and mass loss. If the mass loss is negligible ($c \approx 0$), the variation in time of the envelope is concave [$A''(t) > 0$] and is similar to the familiar exponential decrease of an underdamped oscillatory system. As the energy loss due to the exiting mass becomes more important, we expect the amplitude to decrease in time more rapidly. When the two energy loss mechanisms are comparable ($\varepsilon \approx 1$), the envelope becomes linear. If the flow rate increases even more, so does the rate of energy loss, and we expect the amplitude to decrease in time even more rapidly than linearly, and therefore the envelope becomes convex [$A''(t) < 0$] as in Fig. 3(c).

ACKNOWLEDGMENTS

APPENDIX: MODEL SOLUTION OF THE EQUATION OF MOTION

We wish to find a solution for the equation of motion, Eq. (4). For this purpose we substitute the ansatz in Eq. (15) in Eq. (4) and separately equate the coefficients of $\sin(h(t))$ and $\cos(h(t))$ to zero. We obtain a sufficient condition for the solution of Eq. (4). This procedure yields

$$m(t)(f'' - f(h')^2) + bf' + kf = 0, \tag{A1}$$

and

$$m(t)(2f'h' + fh'') + bfh' = 0. \tag{A2}$$

We then combine Eqs. (11) and (A2) to obtain

$$h'(t) = \left(\frac{k}{m(t)} - \frac{(b + c/2)(b + 3c/2)}{4(m(t))^2} \right)^{1/2}. \tag{A3}$$

Next we define

$$h_0(t) = \int_0^t h'(\tau) \, d\tau. \tag{A4}$$

This integral can be solved analytically, and the solution is

$$h_0(\tau) = \frac{2.\beta}{c} \left[\arctan\left(\sqrt{\frac{1 - \alpha - \tau}{\alpha}} \right) - \left(\sqrt{\frac{1 - \alpha - \tau}{\alpha}} \right) \right], \tag{A5}$$

where $\beta = \frac{1}{2}\sqrt{(b + \frac{1}{2}c)(b + \frac{3}{2}c)}$, $\alpha = \beta^2/m_0 k$, and $\tau = ct/m_0$. When $\tau \to 0$ ($c \to 0$), Eq. (A5) reduces to the familiar equation

$$h_0(t) \to \omega t = \left(\sqrt{\frac{k}{m_0} - \frac{b^2}{4m_0^2}} \right) t, \tag{A6}$$

which is the expected result for the constant mass harmonic oscillator.

The solution to Eq. (4) according to our model is

$$x(t) = A_0 \left(1 - \frac{ct}{m_0} \right)^\varepsilon \sin(h_0(t) + \phi), \tag{A7}$$

where $h_0(t)$ is given by Eq. (A5). If we substitute our solution for $h(t)$ into Eq. (A2), we find that Eq. (A7) is a solution of Eq. (4) as long as the condition,

$$\frac{(b + c/2)(b + 3c/2)}{4(m(t))^2} \ll \frac{k}{m(t)}, \tag{A8}$$

is satisfied. This constraint is equivalent to the well-known condition for underdamped oscillations for constant mass ($c = 0$). Equation (A8) is equivalent to

$$\frac{(b + c/2)(b + 3c/2)}{4k} \ll m(t). \tag{A10}$$

Therefore, we expect our model to become less adequate when the bottle is close to running out of sand.

[a]Author to whom correspondence should be addressed. Electronic mail: sgil@df.uba.ar

[1]K. Y. Shen and Bruce L. Scott, "The hourglass problem," Am. J. Phys. **53** (3), 787–788 (1985).

[2]David Byrd and Gary White, "Alternative theoretical method for motion of a sand-filled funnel experiment," Phys. Teach. **39** (8), 464–465 (2001).

[3]Peter Sullivan and Anna McLoon, "Motion of a sand-filled funnel: An experiment and model," Phys. Teach. **38** (5), 500–502 (2000).

[4]R. A. Serway and R. J. Beichner, *Physics for Scientists and Engineers*, 5th ed. (Brooks/Cole, New York, 1999), Problem 57.

[5]J. Flores, G. Solovey, and S. Gil, "Flow of sand and a variable mass Atwood machine," Am. J. Phys. **71**, 715–720 (2003).

[6]Metin Yersel, "The flow of sand," Phys. Teach. **38** (5), 290–291 (2000).

[7]A. Sommerfeld, *Lectures on Theoretical Physics*, 2nd ed. (Academic, New York, 1964), Vol. I, Chap. I.

[8]D. F. Young, B. R. Munson, and T. H. Okisii, *Fundamentals of Fluid Mechanics*, 2nd ed. (Wiley, New York, 1994), p. 599.

[9]S. Gil and E. Rodríguez, *Física re-Creativa* (Prentice-Hall, Buenos Aires, 2001), p. 91, and ⟨www.fisicarecreativa.com⟩.

[10]J. Copeland, "Work-energy theorem for variable mass systems," Am. J. Phys. **50** (7), 599–601 (1982).